RIMS Kôkyûroku Bessatsu
B21 (2010), 129–147

Mathematical analysis to coupled oscillators system with a conservation law

By

Tomoyuki Miyaji*, Isamu Ohnishi*, Ryo Kobayashi*,
and Atsuko Takamatsu**

§ 1. Introduction

We are interested in bifurcation structure of stationary solution for a 3-component reaction-diffusion system with a conservation law in the following:

$$\begin{cases} \dfrac{\partial u}{\partial t} = \nabla \cdot (D_u \nabla u) + f(u,v) + \delta w, \\ \dfrac{\partial v}{\partial t} = \nabla \cdot (D_v \nabla v) + g(u,v), \\ \dfrac{\partial w}{\partial t} = \Delta\,(D_w w) - f(u,v) - \delta w, \end{cases} \tag{1.1}$$

where the functions $f(u,v)$ and $g(u,v)$ are chosen in such forms that the local oscillator

$$\frac{du}{dt} = f(u,v), \qquad \frac{dv}{dt} = g(u,v) \tag{1.2}$$

can undergo the supercritical Hopf bifurcation. Obviously, the total amount of $u+w$ is conserved under homogeneous Neumann (no-flux) boundary condition and some natural and appropriate conditions.

In [10], they have proposed this system to understand one of the periodic oscillations of the body of the plasmodium of the true slime mold: *Physarum polycephalum.*

Received February 08, 2010. Revised August 05, 2010.
2000 Mathematics Subject Classification(s): 34C23, 37L10, 70K20, 70K50
Key Words: wave bifurcation, coupled oscillators, conservation law, transit process
Supported by JAPAN SUPPORT
*Dept. of Math. and Life Sci.s, Hiroshima University, Hiroshima, 739-8526, Japan.
e-mail: denpaatama@hiroshima-u.ac.jp,
e-mail: isamu_o@math.sci.hiroshima-u.ac.jp,
e-mail: ryo@math.sci.hiroshima-u.ac.jp
**Dept. of Electrical Engineering and Bioscience, Waseda University, Tokyo 168-8555, Japan.
e-mail: atsuko_ta@waseda.jp

The plasmodium of P.P. is an amoeboid multinucleated unicellular organism, which shows various kinds of oscillatory phenomena, for example, thickness of plasmodium, and protoplasmic streaming. Ref.[10] has focused on the oscillation of thickness of the plasmodium. These oscillatory phenomena are supposed to be caused by complicated mechanochemical reactions although the detailed mechanism has not been revealed.

The system (1.1) describes the time-evolution of (u, v, w), which may obtain some spatio-temporal oscillation solutions. We explain the mechanism heuristically in the following: We note that if w does not exist, then the system is a coupled oscillators system with diffusion coupling. The system has temporally oscillation solutions, but we can not observe stable spatially non-uniform oscillation which bifurcates from the homogeneous steady state. It is sure that this system is not appropriate for the model system just as it is.

The plasmodium forms tubular structure which consists of ectoplasm gel outside and endoplasm sol inside. The endoplasm sol streams inside the ectoplasm gel, which is known as protoplasmic streaming. The state variable u and v are defined in the ectoplasm as protoplasm materials included in the ectoplasm gel and biomolecules concentration, respectively. The variable w is defined in the endoplasm as amount of protoplasm which is actively transported by rhythmic contraction of the ectoplasm gel. Note that $u + w$ is a conserved quantity because the total mass of protoplasm is conserved over the time scale considered here. The constant δ is the transportation rate from ectoplasm gel to endoplasm sol, which can also be considered as the stiffness of tubular structure of plasmodium. The variables u and v form a chemical oscillator while w is activated by the chemical oscillator and makes an active flow of endoplasm sol, which is much faster than simple diffusion of chemical materials. Therefore, in this model, $D_w \gg D_u, D_v$ should be assumed.

In biological experiment, for example, if you watch a circular plasmodium propagating on a flat ager surface, you can observe an anti-phase oscillation between the peripheral region and the rear of the plasmodium. Such an oscillation pattern is called *peripheral phase inversion*. In [10], they impose the assumption that D_u **and** δ **depend on the space variable** and reproduce the peripheral phase inversion by numerical simulation. This is very interesting for us too, and we have noticed that the original system **with constant coefficients** is also a mathematically attractive object. This is because this system has the mass conservation law, so that a kind of "degree of freedom" of solutions may be less than the usual 3-component system, in which *wave instability* occurs. We say that the wave instability occurs when a homogeneous state becomes unstable by a pair of nonzero purely imaginary eigenvalues with spatially non-uniform eigenfunctions even though it is stable for spatially uniform perturbation. The wave instability breaks both spatial and temporal symmetries of a homogeneous state, while the (uni-

form) Hopf bifurcation loses only temporal symmetry [6, 11]. Thus it may be possible to explain the peripheral phase inversion without assuming dependency of coefficients on the space variable. Although the linear instability does not imply the existence of stable pattern, in this study, we prove the occurrence of the wave instability under the assumption that all the coefficients are constant.

We consider the system on an interval $\Omega = [0, 1]$ with homogeneous Neumann boundary condition and suppose that $D_u = D_v = \varepsilon, D_w = 1$. We adopt the λ-ω system as a simple local oscillator. In this paper, we use the character "θ" in place of "ω" to avoid confusing w and ω. Therefore we study the following equations:

$$\begin{cases} \dfrac{\partial u}{\partial t} = \varepsilon \dfrac{\partial^2 u}{\partial x^2} + \lambda u - \theta v + \delta w - u(u^2 + v^2), \\ \dfrac{\partial v}{\partial t} = \varepsilon \dfrac{\partial^2 v}{\partial x^2} + \theta u + \lambda v - v(u^2 + v^2), \\ \dfrac{\partial w}{\partial t} = \dfrac{\partial^2 w}{\partial x^2} - \lambda u + \theta v - \delta w + u(u^2 + v^2). \end{cases} \tag{1.3}$$

We can prove mathematically rigorously that the wave instability can occur under natural and appropriate conditions for this system. We will state the main statement of our theorem in the next section. Moreover, in §3, we will show some graphs and figures obtained by numerical simulation in which we observe the Hopf critical points' behavior for each Fourier mode and observe the behavior of solutions near the bifurcation points at which two Fourier modes are made unstable at the same time. We especially notice that this system has a preferable cluster size of synchronization of oscillations, which tends to smaller and smaller as ε goes to 0. It may be interesting that, if the effect by which the synchronized oscillation occurs is too much, then the synchronized cluster is vanishing and a kind of homogenization happens.

We are also interested in spontaneous switching behavior in coupled oscillator systems constructed with *P.polycephalum*[7, 8]. In this biological system, an oscillatory element corresponds to each partial body in the plasmodium. In [8], they reported that a ring of three oscillators showed spontaneous switching among three typical oscillatory states, *rotating(R), partial in-phase(PI)* and *partial anti-phase(PA)*. PI is an oscillation such that two of three oscillators are in-phase. PA is an oscillation such that two of three oscillators are anti-phase. The existence of these three oscillatory patterns is guaranteed by the symmetric Hopf bifurcation theory[4]. However, to understand the spontaneous switching behavior among them, it is necessary to study the further bifurcation structure of them. Recently, Ito and Nishiura studied the bifurcation scenario leading to intermittent switching for three repulsively coupled Stuart-Landau equations[5]. Although the number of the dimensions for their model is 6, it can be reduced to 5. It could be one of the simplest models which shows switching behavior among three or more oscillatory states. We want to consider a more appropriate model for a model of

the plasmodium. Then we study the coupled oscillator system with a conservation law as a toy model. We will show a partial result of this attempt in the section 5.

§ 2. The linearized eigenvalue problem

The equations (1.3) can be written in matrix form as follows:

$$\frac{\partial U}{\partial t} = \left(D\frac{\partial^2}{\partial x^2} + \Lambda \right) U + F(U), \tag{2.1}$$

where $U = (u, v, w)$,

$$D = \begin{pmatrix} \varepsilon & 0 & 0 \\ 0 & \varepsilon & 0 \\ 0 & 0 & 1 \end{pmatrix}, \Lambda = \begin{pmatrix} \lambda & -\theta & \delta \\ \theta & \lambda & 0 \\ -\lambda & \theta & -\delta \end{pmatrix}, F(U) = \begin{pmatrix} -u(u^2+v^2) \\ -v(u^2+v^2) \\ u(u^2+v^2) \end{pmatrix}. \tag{2.2}$$

Remark. It is not necessary for the results in this section that Ω is an interval. Ω is allowed to be N-dimensional bounded domain for $N \geq 1$.

We study the linearized system:

$$\begin{cases} \dfrac{\partial U}{\partial t} = D\Delta U + \Lambda U & \text{in } \Omega, \\ \dfrac{\partial U}{\partial \nu} = 0 & \text{on } \partial\Omega, \end{cases} \tag{2.3}$$

where $U = (u, v, w)$ and ν is the outward unit normal vector on $\partial\Omega$. Now we recall the eigenvalue problem of Laplacian with homogeneous Neumann boundary condition on Ω [1]:

$$\begin{cases} \Delta\psi_n = -k_n^2 \psi_n, \\ \dfrac{\partial \psi_n}{\partial \nu} = 0 & \text{on } \partial\Omega, \end{cases} \tag{2.4}$$

where ν is outward unit normal vector, $-k_n^2$ is an eigenvalue of the Laplacian with Neumann boundary condition, and ψ_n is an eigenvector associated with $-k_n^2$. It holds that $0 = k_0^2 < k_1^2 \leq k_2^2 \ldots$. If $\Omega = [0, 1]$, then we obtain $k_n = n\pi$.

For any integer n, the equations (2.3) admits solutions of the form $U_n(x, t) = V_n e^{\mu_n t}\psi_n(x)$, where $V_n \in \mathbb{R}^3$. Substituting the ansatz into (2.3), we have the eigenvalue problem

$$L_n V_n = \mu_n V_n, \tag{2.5}$$

where the matrix $L_n = \Lambda - k_n^2 D$ is given by

$$L_n = \begin{pmatrix} \lambda - \varepsilon k_n^2 & -\theta & \delta \\ \theta & \lambda - \varepsilon k_n^2 & 0 \\ -\lambda & \theta & -\delta - k_n^2 \end{pmatrix}. \tag{2.6}$$

It is obvious that the eigenvalues of $L_0 = \Lambda$ are identical to that of the local oscillator:

$$\mu_0 = 0, \quad \frac{1}{2}\left(2\lambda - \delta \pm \sqrt{\delta^2 - 4\theta^2}\right).$$

Next, we consider the case of $n \neq 0$. The characteristic polynomial φ_n of L_n is cubic:

$$\varphi_n(\mu) = \mu^3 - \mathrm{tr}L_n\mu^2 + c_n\mu - \det L_n,$$

where

$$\begin{aligned}
\mathrm{tr}L_n &= 2\lambda - \delta - (1+2\varepsilon)k_n^2, \\
c_n &= (\varepsilon^2 + 2\varepsilon)k_n^4 + 2(\delta\varepsilon - \varepsilon\lambda - \lambda)k_n^2 + \lambda^2 + \theta^2 - \delta\lambda, \\
\det L_n &= -k_n^2\{\varepsilon^2 k_n^4 + (\delta\varepsilon^2 - 2\varepsilon\lambda)k_n^2 + \lambda^2 + \theta^2 - \delta\varepsilon\lambda\}.
\end{aligned}$$

It is not impossible to express the solutions of $\varphi_n(\mu) = 0$ explicitly, but it is not suitable for bifurcation analysis. So we take a qualitative approach. We give a sufficient condition for the existence of a pair of complex conjugate eigenvalues of L_n and its real part becomes positive for some n.

We use Gershgorin's theorem[2]:

Theorem 2.1. *Every eigenvalues of an $n \times n$ matrix $A = (a_{ij})$ is contained in at least one of the Gershgorin circles*

$$C_i = \left\{ z \in \mathbb{C}; |z - a_{ii}| \leq \sum_{j \neq i}^{n} |a_{ij}| \right\} \quad (i = 1, \ldots, n). \tag{2.7}$$

Theorem 2.2. *Let $D_1, D_2, \ldots, D_k$ be the disjoint components of the Gershgorin circles. Let D_i be the union of n_i of the circles (so that $\sum n_i = n$). Then D_i contains exactly n_i eigenvalues of A.*

The Gershgorin circles for L_n are

$$\begin{aligned}
C_1^n &= \left\{ z \in \mathbb{C}; |z - (\lambda - \varepsilon k_n^2)| \leq \theta + \delta \right\}, \\
C_2^n &= \left\{ z \in \mathbb{C}; |z - (\lambda - \varepsilon k_n^2)| \leq \theta \right\}, \\
C_3^n &= \left\{ z \in \mathbb{C}; |z - (-\delta - k_n^2)| \leq \lambda + \theta \right\}.
\end{aligned}$$

Since we assume that λ, θ and δ are nonnegative, we can omit the absolute value signs.

Lemma 2.3. *If $C_3^n \subset \{z \in \mathbb{C}; \mathrm{Re}z < 0\}$ and $C_1^n \cap C_3^n = \emptyset$, then L_n has at least one negative real eigenvalue.*

Proof. Obviously, $C_2^n \subset C_1^n$ holds. If $C_1^n \cap C_3^n = \emptyset$, then the disjoint components of the union of the Gershgorin circles of L_n consist of two circles. One contains two circles and the other contains only C_3^n. As we assume $C_3^n \subset \{z \in \mathbb{C}; \mathrm{Re}z < 0\}$, the eigenvalue contained in C_3^n must be negative real value. □

Lemma 2.4. *$C_3^n \subset \{z \in \mathbb{C}; \mathrm{Re}z < 0\}$ and $C_1^n \cap C_3^n = \emptyset$ if and only if*

$$\lambda + \theta < \delta + k_n^2 \tag{2.8}$$

$$2\theta < (1-\varepsilon)k_n^2 \tag{2.9}$$

Proof. The proof is straightforward. $C_3^n \subset \{z \in \mathbb{C}; \mathrm{Re}z < 0\}$ if and only if

$$-\delta - k_n^2 + \lambda + \theta < 0.$$

Hence we obtain $\lambda + \theta < \delta + k_n^2$.

$C_1^n \cap C_3^n = \emptyset$ if and only if

$$-\delta - k_n^2 + \lambda + \theta < \lambda - \varepsilon k_n^2 - \theta - \delta.$$

This is equivalent to $2\theta < (1-\varepsilon)k_n^2$. □

If (2.8) and (2.9) are satisfied, then L_n has at least one negative eigenvalue in C_3^n and the other eigenvalues are in C_1^n.

Next, we consider the extremal values of $\varphi_n(\mu)$. If the minimal value is positive, then $\varphi_n(\mu) = 0$ has a pair of complex conjugate roots.

$$\begin{aligned}\frac{d\varphi_n}{d\mu} &= 3\mu^2 - 2(\mathrm{tr}L_n)\mu + c_n \\ &= 3\mu^2 + 2(\delta - 2\lambda + (1+2\varepsilon)k_n^2)\mu \\ &\quad + (\varepsilon^2 + 2\varepsilon)k_n^4 + 2(\delta\varepsilon - \varepsilon\lambda - \lambda)k_n^2 + \lambda^2 + \theta^2 - \delta\lambda.\end{aligned}$$

The discriminant of $d\varphi_n/d\mu$, Δ_1, is given by

$$\Delta_1 = (1-\varepsilon)^2 k_n^4 + 2(1-\varepsilon)(\delta+\lambda)k_n^2 + \delta^2 + \lambda^2 - \delta\lambda - 3\theta^2.$$

The condition (2.9) gives

$$\begin{aligned}\Delta_1 &> 4\theta^2 + 2(1-\varepsilon)(\delta+\lambda)k_n^2 + \delta^2 + \lambda^2 - 2\delta\lambda + \delta\lambda - 3\theta^2 \\ &= \theta^2 + 2(1-\varepsilon)(\delta+\lambda)k_n^2 + (\delta-\lambda)^2 + \delta\lambda > 0.\end{aligned}$$

Hence $d\varphi_n/d\mu = 0$ has two distinct real roots $\mu_\pm$:

$$\mu_\pm = \frac{1}{3}\left(\mathrm{tr}L_n \pm \Delta_1^{\frac{1}{2}}\right).$$

In other words, $\varphi_n(\mu)$ has the maximal and minimal values. Here remark that

$$\Delta_1 < \left\{(1-\varepsilon)k_n^2 + \delta + \lambda\right\}^2. \tag{2.10}$$

The minimal value $\varphi_n(\mu_+)$ is given by

$$\varphi_n(\mu_+) = -\det L_n + \frac{c_n}{3}\mathrm{tr}L_n - \frac{2}{27}(\mathrm{tr}L_n)^3 - \frac{2}{27}\Delta_1^{\frac{3}{2}}.$$

The inequality (2.10) gives

$$\begin{aligned}\varphi_n(\mu_+) &> -\det L_n + \frac{c_n}{3}\mathrm{tr}L_n - \frac{2}{27}(\mathrm{tr}L_n)^3 - \frac{2}{27}\left\{(1-\varepsilon)k_n^2 + \delta + \lambda\right\}^3 \\ &= \frac{1}{3}\left\{(1-\varepsilon)(2\theta^2 - \delta\lambda)k_n^2 - \delta\lambda^2 - \delta^2\lambda + (2\lambda - \delta)\theta^2\right\} \\ &= \frac{1}{3}\left[\left\{2\lambda - \delta + 2(1-\varepsilon)k_n^2\right\}\theta^2 - \delta\lambda\left\{\delta + \lambda + (1-\varepsilon)k_n^2\right\}\right].\end{aligned}$$

Regard the right-hand side as a quadratic function of θ. Assume

$$2\lambda - \delta + 2(1-\varepsilon)k_n^2 > 0. \tag{2.11}$$

Let

$$\tilde{\theta}_0 = \sqrt{\frac{\delta\lambda\left\{\delta + \lambda + (1-\varepsilon)k_n^2\right\}}{2\lambda - \delta + 2(1-\varepsilon)k_n^2}}.$$

If $\theta > \tilde{\theta}_0$, then $\varphi_n(\mu_+) > 0$. $\varphi_n(\mu) = 0$ has a pair of complex conjugate roots. Especially, $\tilde{\theta}_0$ is a monotonically decreasing function with respect to k_n. If the inequality holds for $n = 1$, then $\varphi_n(\mu) = 0$ has a pair of complex conjugate roots for any $n \geq 1$.

Let $\mu_{1,n}, \mu_{2,n}$ and $\mu_{3,n}$ be three eigenvalues of L_n. Suppose $\mu_{1,n} < 0$ and $\mu_{2,n} = \bar{\mu_{3,n}}$. The coefficient c_n in $\varphi_n(\mu)$ satisfies

$$\begin{aligned}c_n &= \mu_{1,n}\mu_{2,n} + \mu_{2,n}\mu_{3,n} + \mu_{3,n}\mu_{1,n} \\ &= 2\mu_{1,n}(\mathrm{Re}\mu_{2,n}) + |\mu_{2,n}|^2.\end{aligned}$$

Since we have $\mu_{1,n} < 0$, $c_n < 0$ implies $\mathrm{Re}\mu_{2,n} > 0$. We give a sufficient condition for $c_n < 0$. Regard c_n as a quadratic function of k_n^2 and consider its discriminant Δ_2.

$$\begin{aligned}\Delta_2 &= (\delta\varepsilon - \varepsilon\lambda - \lambda)^2 - (\varepsilon^2 + 2\varepsilon)(\lambda^2 + \theta^2 - \delta\lambda) \\ &= -(\varepsilon^2 + 2\varepsilon)\theta^2 + \delta^2\varepsilon^2 + \lambda^2 - \delta\lambda\varepsilon^2.\end{aligned}$$

Let

$$\theta_1^2 = \frac{\varepsilon^2(\delta^2 - \delta\lambda) + \lambda^2}{\varepsilon^2 + 2\varepsilon}.$$

If $\varepsilon > 0$ is sufficiently small, we can choose $\theta^2 < \theta_1^2$. Then we obtain $\Delta_2 > 0$ and the quadratic equation

$$c_n(\xi) \equiv (\varepsilon^2 + 2\varepsilon)\xi^2 + 2(\delta\varepsilon - \varepsilon\lambda - \lambda)\xi + \lambda^2 + \theta^2 - \delta\lambda = 0$$

has two distinct real roots:

$$\xi_{\pm} = \frac{1}{\varepsilon^2 + 2\varepsilon}\left(-\delta\varepsilon + \varepsilon\lambda + \lambda \pm \Delta_2^{\frac{1}{2}}\right).$$

If $\xi_- < k_n^2 < \xi_+$ for $n \in \mathbb{N}$, then $c_n < 0$. Hence we get $\mathrm{Re}\mu_{2,n} > 0$ under the assumption. It is easy to check that $\xi_+ - \xi_-$ is monotonically decreasing with respect to small ε and $\xi_+ - \xi_- \to \infty$ as $\varepsilon \to 0$. In addition,

$$\xi_- = \frac{\lambda^2 + \theta^2 - \delta\lambda}{-(\delta\epsilon - \epsilon\lambda - \lambda) + \Delta_2^{\frac{1}{2}}} \to \frac{\lambda^2 + \theta^2 - \delta\lambda}{2\lambda} \quad \text{as } \varepsilon \to 0.$$

Furthermore, we can get $\xi_+ \to \infty$ as $\epsilon \to 0$. Therefore $\xi_- < k_n^2 < \xi_+$ can be realized for sufficiently small ε.

Therefore we get the following theorem:

Theorem 2.5. *Let $\lambda, \theta, \delta > 0$ and $0 < \varepsilon < 1$. If the following four inequalities hold for an integer n, then L_n has a negative eigenvalue and a pair of complex conjugate eigenvalues:*

$$\lambda + \theta < \delta + k_n^2 \tag{2.12}$$

$$2\theta < (1-\varepsilon)k_n^2 \tag{2.13}$$

$$2\lambda - \delta + 2(1-\varepsilon)k_n^2 > 0 \tag{2.14}$$

$$\sqrt{\frac{\delta\lambda\left\{\delta + \lambda + (1-\varepsilon)k_n^2\right\}}{2\lambda - \delta + 2(1-\varepsilon)k_n^2}} < \theta \tag{2.15}$$

Furthermore, under the above assumptions, if ε is sufficiently small, then L_n has a pair of complex conjugate eigenvalues with positive real part.

Remark. If the inequalities hold for $n = 1$, then L_n has a negative eigenvalue and a pair of complex conjugate eigenvalues for $n \geq 1$. Especially, it should be noted that even if the real part of 0-mode eigenvalue is negative ($2\lambda < \delta$), then that of n-mode can be positive for some $n \geq 1$. This implies that the wave instability occurs.

Remark. The conditions (2.12)-(2.15) can be understood as follows. (2.12) means that the transportation rate between sol and gel is needed to be sufficiently large, and higher modes helps it. (2.14) means that if flow in the tube and effects of higher modes are sufficiently large, then it is possible to destabilize the homogeneous steady state. (2.13) and (2.15) implies that the frequency of local oscillators should be contained in some appropriate range determined by the effects of transportation, flow and higher modes.

Remark. If $D_u = D_v = D_w = d > 0$, the problem is very easy. The eigenvalues of L_n are given by

$$\mu_n = -dk_n^2, \quad \frac{1}{2}\left(2\lambda - \delta - 2dk_n^2 \pm \sqrt{\delta^2 - 4\theta^2}\right).$$

According to the monotonicity of the eigenvalues of Laplacian, 0-mode is the most unstable. Therefore, in this case, wave instability does not occur as the first bifurcation.

Remark. The same result holds when we impose the periodic boundary conditions. Let Ω be the set $\prod_{j=1}^{n}(0, L_j) \subset \mathbb{R}^n, L_j > 0$. We denote by Γ_j, Γ_{j+n} the following faces of $\Gamma = \partial\Omega$:

$$\Gamma_j = \Gamma \cap \{x_j = 0\}, \quad \Gamma_{j+n} = \Gamma \cap \{x_j = L_j\}, \quad j = 1, 2, \ldots, n.$$

Consider the eigenvalue problem

$$\begin{cases} \Delta\psi = \lambda\psi, & \text{in } \Omega, \\ \psi|_{\Gamma_j} = \psi|_{\Gamma_{j+n}}, & j = 1, 2, \ldots, n \\ \dfrac{\partial\psi}{\partial x_j}\Big|_{\Gamma_j} = \dfrac{\partial\psi}{\partial x_j}\Big|_{\Gamma_{j+n}}. \end{cases} \tag{2.16}$$

The eigenvalues and eigenfunctions are well known in this case[9]:

$$\begin{cases} \lambda_0 = 0, \psi_0 = \dfrac{1}{\sqrt{|\Omega|}}, \quad |\Omega| = L_1 \cdots L_n, \\ \lambda_k = -4\pi^2 \left(\dfrac{k_1^2}{L_1^2} + \cdots \dfrac{k_n^2}{L_n^2}\right), \\ \psi_k = \sqrt{\dfrac{2}{|\Omega|}} \cos 2\pi \dfrac{kx}{L}, \quad \tilde{\psi}_k = \sqrt{\dfrac{2}{|\Omega|}} \sin 2\pi \dfrac{kx}{L}, \end{cases} \tag{2.17}$$

where $k \in \mathbb{N}^n$ and $kx/L = k_1x_1/L_1 + \cdots + k_nx_n/L_n$. Therefore we obtain a monotonically decreasing sequence of eigenvalues from zero to $-\infty$ as in the case of Neumann boundary conditions.

§ 3. Numerical simulations

In this section, we briefly show the results obtained by numerical simulation. The system (1.3) with zero-flux boundary condition was solved numerically in one spatial dimension using a explicit finite difference method. To calculate the eigenvalues of each matrix L_n, we employed the QR method.

We have already known that the eigenvalues of L_n are one negative and a pair of complex conjugate. Therefore we focus on the real parts of the complex eigenvalues μ_n to study the bifurcation structure.

The constant θ is supposed to be $\theta = 1$.

Figure 1 shows each Hopf bifurcation curve($\mathrm{Re}\mu_n = 0$) for corresponding Fourier mode in the parameter space (δ, λ) for some fixed ε. Here ε is the diffusion coefficient of u and v. Small ε leads to spatially non-uniform Hopf bifurcation, that is, wave instability. If ε is chosen smaller, then the higher Fourier mode becomes unstable as the first bifurcation. Hence it can be said that fast diffusion of w plays an important role for the emergence of the wave instability in (1.3). As shown in Figure 1, each of Hopf bifurcation curves can intersect. These intersections imply wave-wave interactions.

Figure 2 shows each Hopf bifurcation curve($\mathrm{Re}\mu_n = 0$) for corresponding Fourier mode in the parameter space (δ, ϵ) for some fixed λ. $\mathrm{Re}\mu_0$ is positive in the left region of the vertical line and negative in the right. $\mathrm{Re}\mu_n$ is positive in the lower region of each slope and negative in the upper region. This figure also suggests that fast diffusion of w (small ϵ) and effective transportation between gel and sol (large δ) are crucial for the wave instability.

Figure 3 shows the behavior of the most unstable mode number as $\varepsilon \to 0$. The parameters are chosen so that $\mathrm{Re}\mu_0 = 0$. At $\varepsilon = 1$, 0-mode eigenvalue is the most unstable. However, the most unstable mode number changes successively as ε approaches to zero.

Figure 4 shows stable standing wave solutions. The 2-mode standing wave solution is very similar to peripheral phase inversion behavior of plasmodium. Of course, standing waves with different wave-length can be observed for corresponding parameters. Furthermore, spatio-temporal patterns arising from the interaction between wave instabilities of different modes can be observed (See Figure 5). It will take the form $\mathrm{Re}\left(z_1 \exp(i\omega_1 t)\cos(\pi x)\phi_1 + z_2 \exp(i\omega_2 t)\cos(2\pi x)\phi_2\right)$ at the linear approximation, where $i\omega_1$ and $i\omega_2$ are critical eigenvalues corresponding to 1-mode and 2-mode eigenfunctions $\cos(\pi x)\phi_1, \cos(2\pi x)\phi_2$, respectively. Remark that we do not only need linear stability analysis, but also nonlinear analysis such as center manifold reduction in order to understand bifurcation structure.

§ 4. Discussion, Conclusion, and Future works

In the system (1.3), the wave instability plays a central and crucial role for pattern formation. It turned out the pattern like peripheral phase inversion to be naturally included in the system. In addition, the system can exhibit many other spatio-temporal structures. Therefore, from the viewpoint of our study, we can interpret the work in [10] as follows: To understand the behavior of the plasmodium system mathematically,

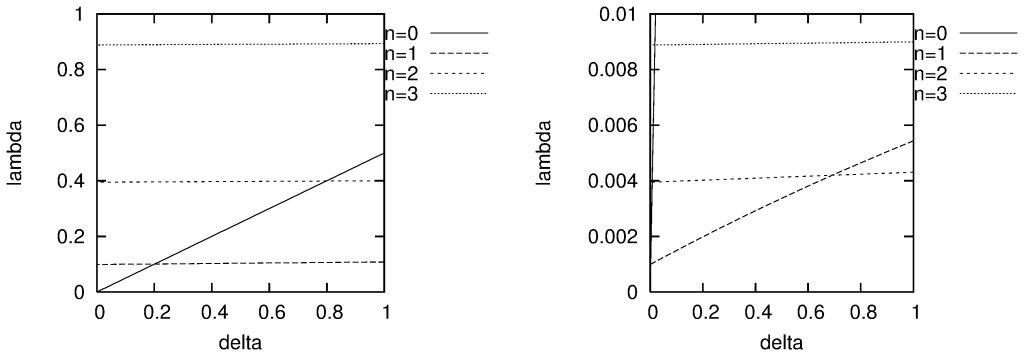

Figure 1. Hopf bifurcation curves in (δ, λ)-plane. Parameter: $\varepsilon = 0.01$(left),$\varepsilon = 0.0001$(right).

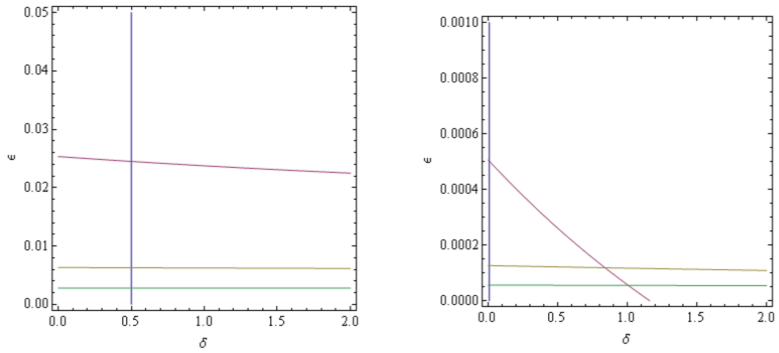

Figure 2. Hopf bifurcation curves in (δ, ϵ)-plane. Parameter: $\lambda = 0.25$(left),$\lambda = 0.005$(right). The curves corresponding to $\mathrm{Re}\mu_n = 0$ for $n = 0, 1, 2, 3$ are drawn. The vertical line is 0-mode curve. Horizontal lines are 1-mode, 2-mode, and 3-mode from upper to lower, respectively, which incline toward lower right.

they crushed the structures in which the solution did not behave like the plasmodium system of *Physarum polycephalum* by considering spatially dependence of coefficients naturally. As a result, they succeeded to construct the mathematical model which was better to reproduce behavior of the plasmodium system cleverly.

In this study, $D_u = D_v$ is assumed. If $D_u \neq D_v$, the Turing instability might be caused. In [11], they study the pattern formation arising from the interaction between Turing and wave instability in 3-component oscillatory reaction diffusion system. Their system does not satisfy any conservation law. In the future, we would like to consider that how different the structure of bifurcations is ? On the other hand, the homogenization of the synchronized oscillation cluster size, which has been already mentioned in §1, is another mathematically interesting problem. We try to make this be a mathematical result.

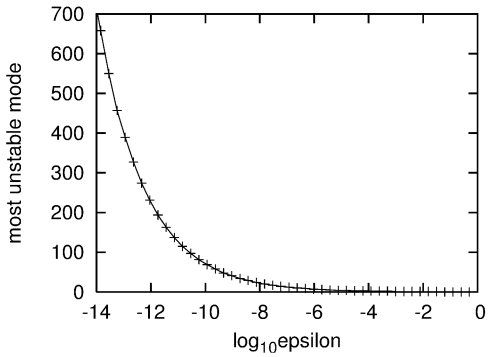

Figure 3. The most unstable mode number increases as $\varepsilon \to 0$.The parameters are $(\lambda, \theta, \delta) = (0.5, 1, 1)$.The horizontal line indicates $\log_{10} \varepsilon$ and the vertical line does the mode number which has the most positive eigenvalue for fixed ε.

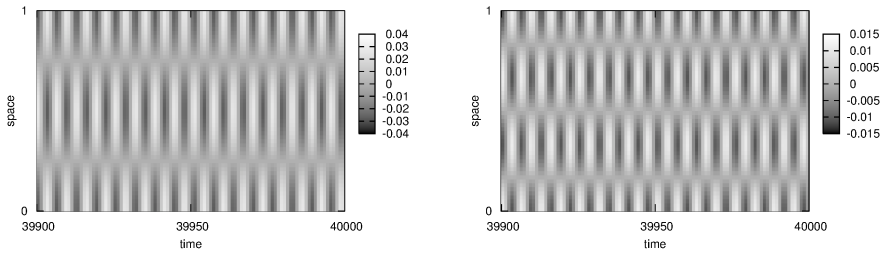

Figure 4. Stable standing wave solutions. The left is 2-mode oscillation for $(\lambda, \theta, \delta, \varepsilon) = (0.005, 1, 1, 0.001)$. The right is 3-mode oscillation for $(\lambda, \theta, \delta, \varepsilon) = (0.0004, 1, 1, 0.000003)$

§ 5. Three oscillators system with $\mathbf{D}_3$ symmetry

Equations. In this section we study a coupled oscillator system with three oscillators in ring, as in Figure 6. We consider the following system:

$$
\begin{cases}
\dfrac{du_i}{dt} = \lambda u_i - \theta v_i + \delta w_i - (u_i - \alpha v_i)(u_i^2 + v_i^2) + \varepsilon(u_{i+1} + u_{i-1} - 2u_i), \\
\dfrac{dv_i}{dt} = \theta u_i + \lambda v_i - (\alpha u_i + v_i)(u_i^2 + v_i^2) + \varepsilon(v_{i+1} + v_{i-1} - 2v_i), \\
\dfrac{dw_i}{dt} = -\lambda u_i + \theta v_i - \delta w_i + (u_i - \alpha v_i)(u_i^2 + v_i^2) + D_w(w_{i+1} + w_{i-1} - 2w_i),
\end{cases} \tag{5.1}
$$

where $i = 0, 1, 2$ and the indices are taken mod 3. The coupling strengths ε and D are non-negative. Let the ratio between two coupling strengths be $r = \varepsilon / D_w$. Assume $D_w = 1$ throughout this paper. The parameter α is an amplitude dependency on phase velocity. We will consider the two-parameter bifurcation in (r, α). If r is near 1, as

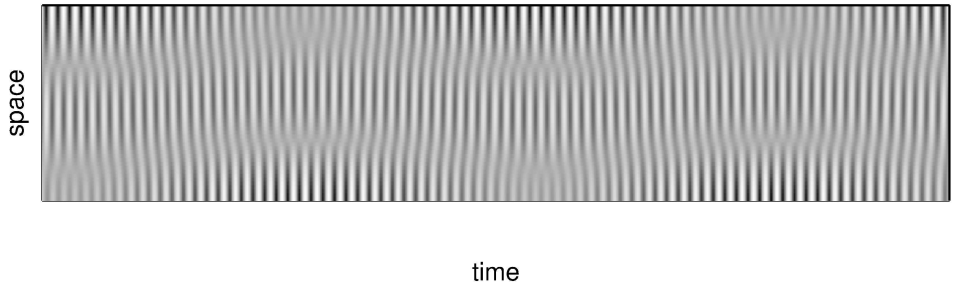

Figure 5. Mode interaction between 1-mode and 2-mode.

we shall see later, the system shows in-phase oscillation($U_0 = U_1 = U_2$). However, if r becomes sufficiently small, nonuniform oscillation occurs. Then local oscillators (u_i, v_i) are coupled very weakly or are not coupled directly, and the fast diffusive variables w_i mediate the coupling between local oscillators. It corresponds to the situation in which each cell of plasmodium is coupled by the tube.

The individual oscillators are denoted by column vector $U_i = (u_i, v_i, w_i)^t$. Then the system (5.1) is written in matrix form as follows:

$$\frac{d}{dt}U_i = \Lambda U_i + F(U_i) + K\left(U_{i+1} + U_{i-1} - 2U_i\right), \tag{5.2}$$

where the matrix Λ and the function F are given by (2.2) and $K = \mathrm{diag}(\varepsilon, \varepsilon, D_w)$ is a diagonal matrix.

Obviously, the sum $\sum(u_i + w_i)$ is conserved throughout the time-evolution. We assume $\sum(u_i + w_i) = 0$. Then (5.1) has a trivial equilibrium point $U_0 = U_1 = U_2 = 0$.

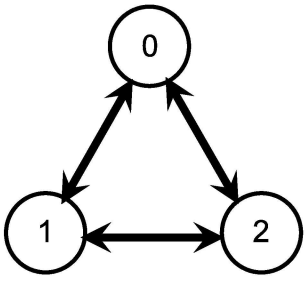

Figure 6. A ring of three oscillators.

Hopf bifurcation of trivial equilibrium point. First, we consider the Hopf bifurcation of trivial equilibrium point. We are assuming that the coupling of oscillators is symmetric, that is, invariant under interchanging the oscillators. Therefore the entire system has $\mathbf{D}_3$ symmetry.

Consider the discrete Fourier transform

$$\hat{U}_k = \frac{1}{3}\sum_{k=0}^{2} U_j \bar{W}^{jk}, \quad k \in \mathbb{Z},$$

where $W = e^{\frac{2\pi i}{3}}$ and hence $\bar{W} = e^{-\frac{2\pi i}{3}}$. $\hat{U}_k$ is the oscillatory component of U_j with wave number k. $\hat{U}_0$ is a spatially uniform component, and $\hat{U}_1, \hat{U}_2$ correspond to spatial patterns. The linearized equation of (5.1) about the trivial equilibrium point is decomposed into that of each oscillatory component,

$$\frac{d\hat{U}_0}{dt} = \Lambda\hat{U}_0, \quad \frac{d\hat{U}_1}{dt} = (\Lambda - 3K)\hat{U}_1, \quad \frac{d\hat{U}_2}{dt} = (\Lambda - 3K)\hat{U}_2.$$

Theorem 4.1 from Chap.XVIII in [4] provides a list of possible oscillatory patterns. When (5.1) undergoes the Hopf bifurcation, either of the following two cases occurs:

1. The Hopf critical eigenvalues arise from the matrix Λ, and in-phase oscillation occurs.

2. The Hopf critical eigenvalues arise from the matrix $\Lambda - 3K$, and it gives rise to three branches of symmetry-breaking oscillations:

   - rotating(R): the solution's trajectory is invariant under rotation,
   - partial in-phase(PI): two of three oscillators are synchronized with same phase,
   - partial anti-phase(PA): two of three oscillators are synchronized with anti-phase.

Because the matrices Λ and $\Lambda - 3K$ correspond to L_0 and L_1 defined by (2.6) with $k_1^2 = 3$, we can apply Theorem 3 in §2. Therefore, if ε is sufficiently small, the second case does occur. In this case, each oscillator is *inactive*, that is, each oscillator does not have limit cycle when there is no coupling.

Inactive case. Next, we consider the inactive case ($2\lambda < \delta$). The parameters are set as

$$\lambda = 0.01, \quad \theta = 1.0, \quad \delta = 0.025.$$

We follow the branches of periodic solutions by using of AUTO. Figure 7 is a two-parameter bifurcation diagram. In region E, trivial equilibrium point is stable. It undergoes the Hopf bifurcation at $r \approx 0.00291$ and three branches of solutions occur. R is stable while PI and PA are unstable. This Hopf bifurcation points are irrelevant to α. On the curve shown in figure, rotating solutions undergo torus bifurcation. In region N, the system shows non-periodic oscillations. Note that this diagram is incomplete. Figure

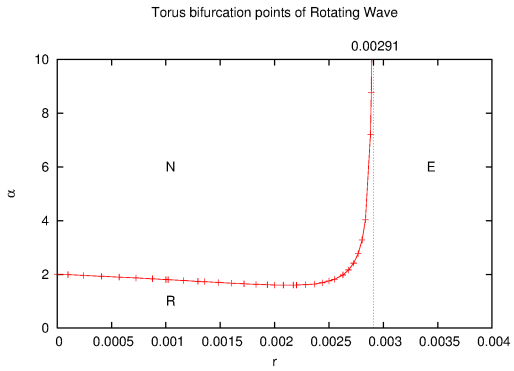

Figure 7. A two-parameter bifurcation diagram for $(\lambda, \theta, \delta) = (0.01, 1.0, 0.025)$. In region E, trivial equilibrium point is stable. The vertical line near $r = 0.00291$ is the Hopf bifurcation points. In most part of region R, the rotating solutions are stable. On the curve shown in figure, it undergoes torus bifurcation. In region N, the system shows non-periodic oscillations.

7 shows only bifurcations of rotating solution. However, as shown in [5], secondary Hopf bifurcation of partial anti-phase could be important. In fact, it is possible to observe the coexistence of periodic and non-periodic oscillation in region R near the torus bifurcation curve. It might be caused by secondary Hopf bifurcation of *PA* or *PI*. Figure 8 shows a time series of rotating solution for $\alpha = 0.0$ and Figure 9 is that of unstable *PA* and *PI*. Figure 10 shows a non-periodic orbit for $\alpha = 2.0$.

Active(self-oscillating) case. Next, we consider the *active* case($2\lambda > \delta$), that is, each element has a limit cycle even if there is no coupling. The parameters are set as

$$\lambda = 0.04, \quad \theta = 1.0, \quad \delta = 0.025.$$

In this case, if r is large, each oscillator tends to in-phase synchronization. For example, if we fix $r = 1$ and increase λ from 0, the first case of $\mathbf{D}_3$ symmetric Hopf bifurcation occurs at $\lambda = \delta/2$. Or, as shown in [3], if the coupling matrix K is proportional to the identity matrix and the local oscillator gives periodic solution, then the uniform oscillation is stable. As r decreases, the synchronous state loses its stability. Figure 11 shows some orbits observed in active case. If $\alpha = 0$, the stable in-phase synchronized state loses its stability at $r \approx 0.0036$. This critical value decreases as the parameter α increases. Figure 12 shows the bifurcation points of synchronized state. It is obtained by following the synchronized solution for each fixed value of α by AUTO.

Conclusion We have presented a partial result of the bifurcation structure of three-oscillator system with conservation law. In inactive case, three non-uniform oscillatory

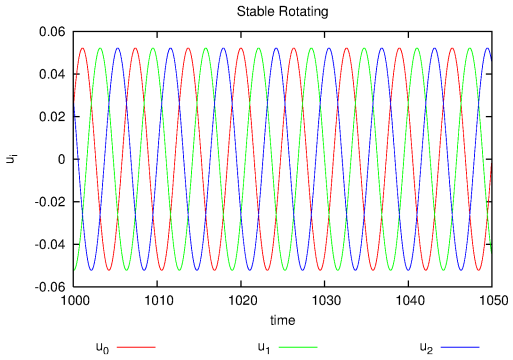

Figure 8. Time series of a stable rotating solution for $(\lambda, \theta, \delta, \alpha) = (0.01, 1.0, 0.025, 0.0)$. The values of u_0, u_1 and u_2 are indicated. The period of each oscillator is $T \approx 6.3$ and the phase difference is about 2.1.

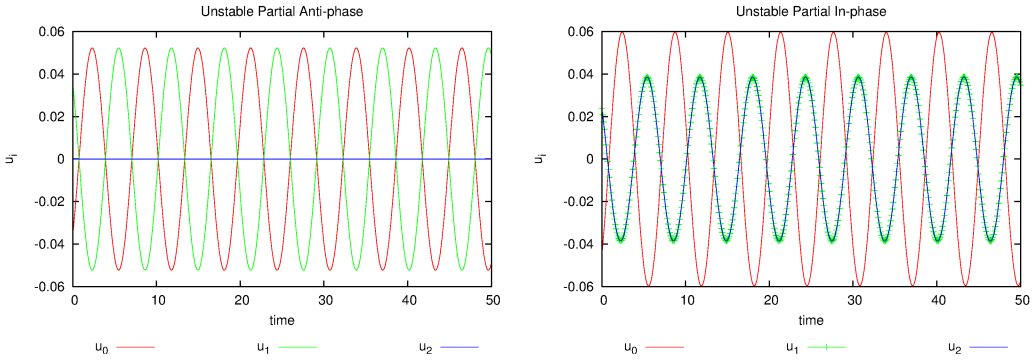

Figure 9. Time series of unstable solutions for $(\lambda, \theta, \delta, \alpha) = (0.01, 1.0, 0.025, 0.0)$. The values of u_0, u_1 and u_2 are indicated. Left:partial-anti-phase. u_0 and u_1 are anti-phase and u_2 is in death-mode ($u_2 = 0$). Right:partial in-phase. In this figure, u_1 and u_2 are in-phase.

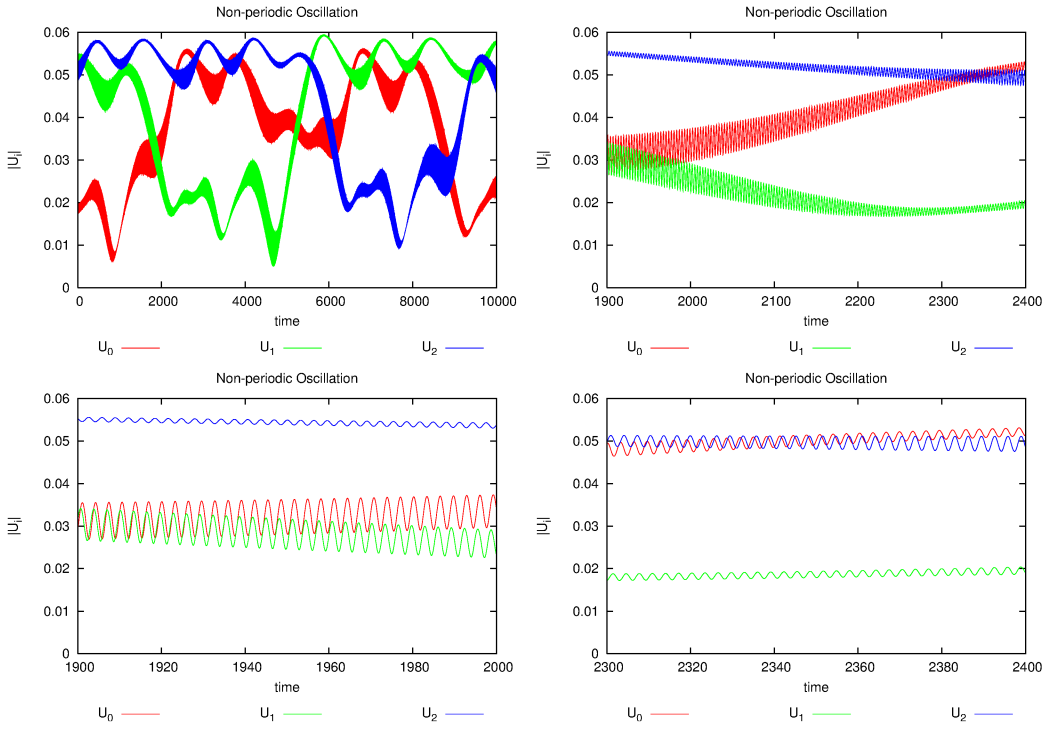

Figure 10. Time series of a non-periodic orbit for $(\lambda, \theta, \delta, \alpha) = (0.01, 1.0, 0.025, 2.0)$. The standard Euclidean norms of vectors U_0, U_1 and U_2 are indicated.

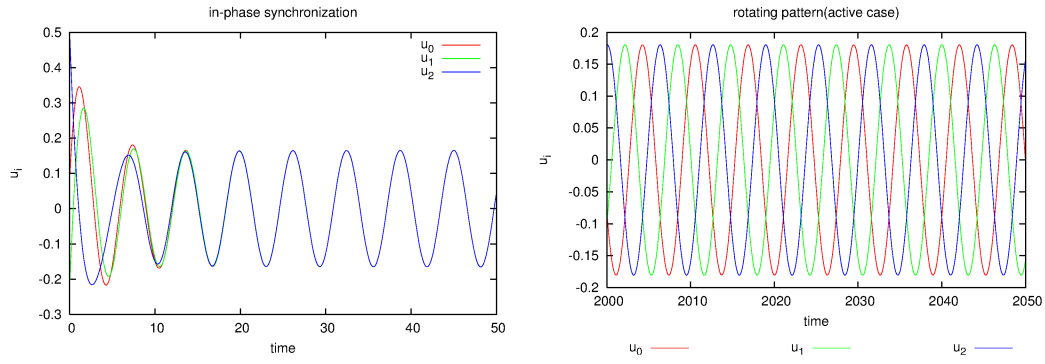

Figure 11. Time series of solutions for $(\lambda, \theta, \delta, \alpha) = (0.04, 1.0, 0.025, 0.0)$. The values of u_0, u_1 and u_2 are indicated. Left: an orbit tends to the synchronized state for $r = 0.1$. Right: rotating solution for $r = 0.002$.

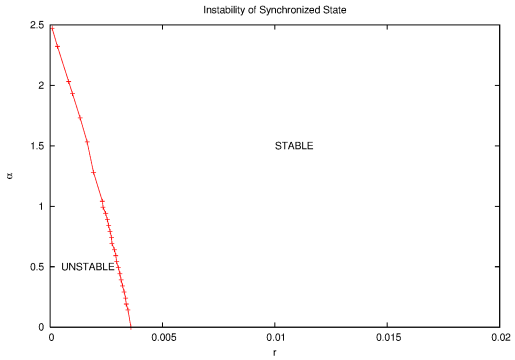

Figure 12. The bifurcation points of synchronized state in (r, α)-plane. "STABLE" and "UNSTABLE" means the stability of synchronized states.

patterns bifurcate at the Hopf bifurcation point. It is derived from the group theoretical bifurcation theory as shown in [4] and is also understood as an analogy of the symmetry-breaking induced by wave instability in our reaction-diffusion system with conservation law. Further bifurcations of these patterns lead to non-periodic oscillation.

It is expected that the result similar to the case of three repulsively coupled Stuart-Landau equations studied in [5] is obtained. The switching behavior is understood as a chaotic itinerancy which shows chaotic transitions among low dimensional ordered states. In that paper, they have clarified a bifurcation scenario which generates intermittent switching behavior. In inactive case, they have observed the following route to chaos: trivial equilibrium $\rightarrow$ partial anti-phase $\rightarrow$ S_2 torus $\rightarrow$ S_3 chaos, where S_2 torus is an attractor corresponding to quasi-periodic motion and it is invariant under permutation by S_2 group action. S_3 chaos is a chaotic attractor invariant under permutation by the action of S_3. In active case, the route consists of two parts: the first part is the creation of chaotic attractor through the period-doubling cascade:S_2 torus $\rightarrow$ S_1 torus S_1 chaotic attractor. The second part is two successive attractor-merging crises: S_1 chaotic attractor $\rightarrow$ S_2 chaotic attractor $\rightarrow$ S_3 chaos. However, our result for three-oscillator system is incomplete. We have observed the occurrence of symmetry-breaking oscillation by equivariant Hopf bifurcation, and non-periodic orbit after the destabilization of rotating wave. Although these solutions may be the first part of route to S_3 chaos, we need a more detailed analysis from both mathematical and numerical viewpoints.

To understand the switching behavior in the biological coupled oscillator system, we might have to propose a more appropriate mathematical model. In (5.1), each oscillator consists of three variables and the coupling with other oscillator is mediated by w_j, which has large coupling constant and it corresponds to tube structure of Physarum. This third variable enables the occurrence of spatially non-uniform oscillation although

each oscillator is diffusively coupled. Since each oscillator is diffusively coupled, it seems attractive coupling. However, the fast component w makes the system behave like a repulsively coupled Stuart-landau equations. It results in spatially non-uniform stable oscillations. The character that the variable with fast diffusion mediates the coupling is essential.

Acknowledgement

The first author was adopted as a Research Fellow of the Japan Society for the Promotion of Science and supported by Grant-in-Aid for JSPS Fellows, No.20.3310, mainly when he concentrated to perform this work. The second author is partially supported for this work by Grant-in-Aid No.22540136 in JSPS. We moreover express our deep appreciation to our refree to this work for their useful comments and adequate indications.

References

[1] Courant, R. and Hilbert, D.: Methods of Mathematical Physics, Interscience Publishers, New York(1953).
[2] Franklin, J.N.: Matrix Theory, Prentice Hall, Englewood Cliffs, NJ (1968).
[3] Fujisaka, H. and Yamada, T.: Stability Theory of Synchronized Motion in Coupled-Oscillator Systems, Prog.Theor.Phys. **69** (1983), pp.32-47.
[4] Golubitsky, M., Stewert, I. and Schaeffer, D. G.: Singularities and Groups in Bifurcation Theory Vol.II, Springer-Verlag, Berlin(1988).
[5] Ito, K. and Nishiura, Y.: Intermitent switching for three repulsively coupled oscillators, Phys.Rev.E **77** (2008), 036224.
[6] Ogawa, T.: Degenerate Hopf instability in oscillatory reaction-diffusion equations, DCDS Supplements, Special volume (2007), pp.784-793.
[7] Takamatsu, A., Tanaka, R., Yamada, H., Nakagaki, T., Fujii, T. and Endo, I.: Spatiotemporal Symmetry in Rings Coupled Biological Oscillators of *Physarum* Plasmodial Slime Mold, Phys.Rev.Lett. **87** (2001), 078102.
[8] Takamatsu, A.: Spontaneous switching among multiple spatio-temporal patterns in three-oscillator systems constructed with oscillatory cells of true slime mold, Physica D **223** (2006), pp.180-188.
[9] Temam, R.: Infinite-Dimensional Dynamical Systems in Mechanics and Physics, Second Edition, Springer-Verlag (1997).
[10] Tero, A., Kobayashi, R. and Nakagaki, T.: A coupled-oscillator model with a conservation law for the rhythmic amoeboid movements of plasmodial slime molds, Physica D **205** (2005), pp.125-135.
[11] Yang, L., Dolnik, M., Zhabotinsky, A. M. and Epstein, I. R.: Pattern formation arising from interactions between Turing and wave instabilities, J. Chem. Phys., 117 (2002), pp.7259-7265.